Photonics **2015**, *2*, 342-354; doi:10.3390/photonics2020342

OPEN ACCESS

photonics

ISSN 2304-6732

www.mdpi.com/journal/photonics

Article

Harmonic Mode-Locked Fiber Laser based on Photonic Crystal Fiber Filled with Topological Insulator Solution

Yu-Shan Chen, Pei-Guang Yan, Hao Chen, Ai-Jiang Liu and Shuang-Chen Ruan *

Shenzhen Key Laboratory of Laser Engineering, Key Laboratory of Advanced Optical Precision Manufacturing Technology of Guangdong Higher Education Institutes, College of Optoelectronic Engineering, Shenzhen University, Shenzhen, Guangdong 518060, China;
E-Mails: chanyushan2@gmail.com (Y.-S.C.); yanpg@szu.edu.cn (P.-G.Y.); wmengxjy@163.com (H.C.); andrelau200@ gmail.com (A.-J.L.)

***** Author to whom correspondence should be addressed; E-Mail: scruan@szu.edu.cn; Tel.: +86-139-2529-4507; Fax: +86-755-2653-4062.

Received: 28 February 2015 / Accepted: 29 March 2015 / Published: 3 April 2015

Abstract: We reported that the photonic crystal fiber (PCF) filled with TI:Bi_2Te_3 nanosheets solution could act as an effective saturable absorber (SA). Employing this TI-PCF SA device; we constructed an ytterbium-doped all-fiber laser oscillator and achieved the evanescent wave mode-locking operation. Due to the large cavity dispersion; the fundamental mode-locking pulse had the large full width at half maximum (FWHM) of 2.33 ns with the repetition rate of ~1.11 MHz; and the radio frequency (RF) spectrum with signal-to-noise ratio (SNR) of 61 dB. In addition; the transition dynamics from a bunched state of pulses to harmonic mode-locking (HML) was also observed; which was up to 26th order.

Keywords: Topological Insulator; photonic crystal fiber; mode-locked fiber laser; evanescent wave; harmonic mode-locking

1. Introduction

In the past decade, passively mode-locked fiber lasers have been extensively investigated due to its simplicity and compactness [1–3]. The high repetition rates of passively mode-locked fiber lasers with subnanosecond to picosecond pulses have potential applications in many fields, including high speed optical communication, optical frequency metrology [4,5]. As an important technique to increase the pulse repetition rate, the relevant harmonic mode locking (HML) fiber lasers have been a growing

research region. To date, most of the previous works on HML were related to the nonlinear polarization rotation (NPR) [6–9] and nonlinear amplifying mirrors (NALMs) technique [10]. However, mode-locked fiber lasers based on NPR and the NALM technique are intrinsically environmentally unstable. Therefore, researchers have strong motivations investigate HML in passively mode-locked fiber lasers by real saturable absorbers (SAs) [11–16], such as semiconductor saturable absorbers (SESAM), single-walled carbon nanotube (SWNT) and graphene. However, these SAs also possess some inherent drawbacks. SESAMs have a narrow broadband response and require complex fabrication process and expensive equipment. SWNTs are also restricted by their diameter-dependent response spectral range, and suffered with a relatively high non-saturable loss for broadband operation. In addition, single-layer graphene is an intrinsic ultra-broadband SA, but its modulation depth is often low (typically <1% per layer [17]). Also, grapheme powder [18] and nanoscale charcoal powder [19] were employed as nano-scale saturable absorbers effectively achieve mode-locked.

Recently, another new type of Dirac material, topological insulators (TIs), which have become one of the most interesting research topics in condensed-matter physics [20,21]. At the same time, they have been successfully utilized as SA for the realization of mode-locking [22–41]. TISA could be fabricated by the mechanical exfoliation, the molecular beam epitaxy (MBE) growth, the vapor-liquid-solid growth, chemical exfoliation, the mechanical triturating and the filmy method in polyvinyl alcohol [25,42–44]. In most of recent studies, the nanostructured TIs are typically deposited onto the fiber ferrule [23,28,29,45]. However, the interaction length of the nanostructured TI with light is limited due to large material losses. The SA device based on the evanescent wave interaction is another effective approach to achieve mode-locked fiber laser [22,32,46,47]. Nevertheless, the microfiber-based SAs are very frangible with the disadvantage of high insertion loss (IL) and short interaction length [27], the side-polished-fiber-based SAs exhibit polarization dependent loss due to centrosymmetric structure [48]. Photonic crystal fiber (PCF) [49], characterized with regular air holes along fiber length, has been utilized as platform of SA for evanescent wave interaction by filling the nanoparticles into cladding holes [50–52]. More recently, the HML erbium-doped fiber lasers based on TISA has also been investigated experimentally [27,53]. However, no previous experiments have reported the HML in an ytterbium-doped all-fiber laser oscillator in the all-normal dispersion regime based on TI-filled PCF (TI-PCF) SA. In addition, it has been demonstrated that introducing proper high nonlinear effect into the laser cavity was favorable for generating harmonic mode locking (HML) pulses [27]. The small-core PCF usually has a higher nonlinearity than conventional single mode fiber (SMF). Meanwhile, TIs possess giant third order nonlinear optical property (~10–14 m^2/W) [54]. Therefore, the TI-PCF type of saturable absorber can introduce larger nonlinearity, benefiting for the generation of HML pulses.

In this paper, we reported that the PCF filled with TI:Bi_2Te_3 nanosheets solution could act as an effective SA. Employing this TI-PCF SA device, we constructed an ytterbium-doped all-fiber laser oscillator and achieved the evanescent wave mode-locking operation. Fundamental mode-locking and harmonic mode-locking (HML) up to 26th order were demonstrated.

2. Sample Preparation and Experimental Setup

The scanning electron micrographs (SEM) of the PCF were shown in Figure 1. The total outer diameter was measured about 127 μm. The central core, fabricated by replacing the central air hole with a silica rod, had a diameter of 9.5 μm. The diameter and pitch of air holes were 5.62 μm and 8.3 μm, respectively. The fundamental and 2nd mode distribution were calculated and shown in the insets of Figure 1b. The guided light in fundamental mode could interact with the TI:Bi_2Te_3 nanosheets in solution through the evanescent wave. Acting as the platform of SA, it should be pointed out that the PCF could eliminate the higher order mode in laser cavity under the following conditions: (1) the PCF was deliberately bent in our experiment tightly to suppress the high order modes; (2) Both ends of the PCF was spliced with SMF-28 fiber to avoid the excitation of high order mode. The mode field diameter (MFD) of the PCF was measured ~8.7 μm at 1310 nm. And its attenuation and dispersion parameter at 1060 nm were measured to be 2.2 dB/km and –20.5 ps/km/nm, respectively.

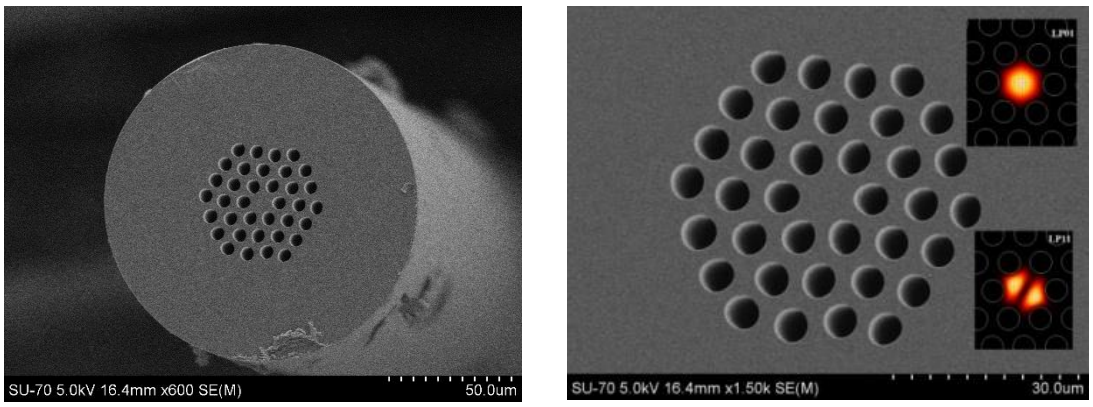

(**a**) (**b**)

Figure 1. The structure of PCF. (**a**) the whole cross section, (**b**) the enlarged microstructured region. The insets in (**b**) were calculated mode distribution of fundamental mode and 2nd mode.

The TI:Bi_2Te_3 nanosheets were synthesized with a low cost and convenient approach based on the hydrothermal intercalation/exfoliation method. Figure 2a showed the SEM of TI:Bi_2Te_3 nanosheets. The TI solution was shown in the inset of Figure 2b, which fabricated by dispersing 0.25 mg samples into 4 mL deionized water, and homogenized with 30-minites ultrasonication. The transmission spectrum of the solution was measured from 1000 nm to 1700 nm using an optical spectrometer (Perkinelmer Lambda 7500), and the linear-transmission ratio was ~43% at 1060 nm, as shown in Figure 2b.

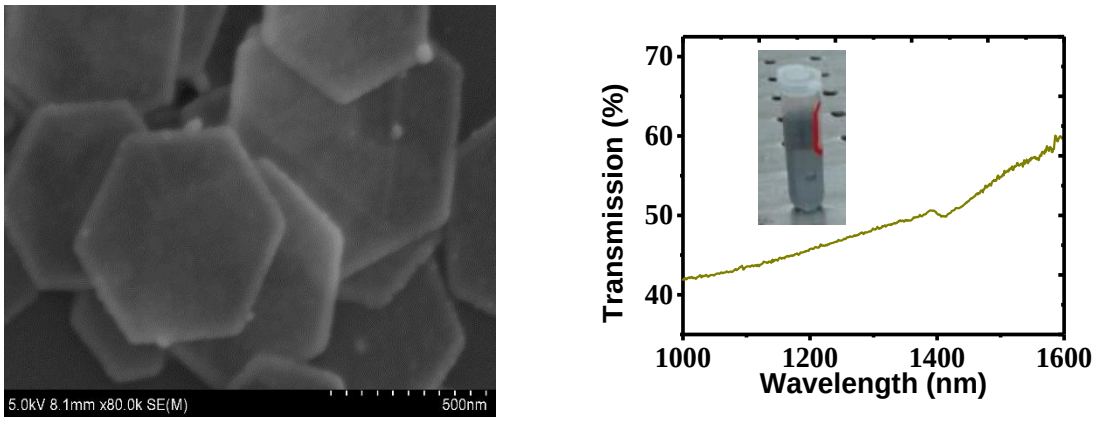

(**a**) (**b**)

Figure 2. (**a**) SEM of TI:Bi_2Te_3 nanosheets; (**b**) The transmission spectrum of the solution.

The TI solution was pulled into the air holes of PCF by an injector. The TI-PCF SA device had a length of 8cm with each end spliced with SMF-28 fiber. The measured insertion loss (IL) was only ~0.45 dB. To check the TI nanosheets really modulated the guided light in PCF, the saturable absorption property of the TI-PCF SA was measured and shown in Figure 3.

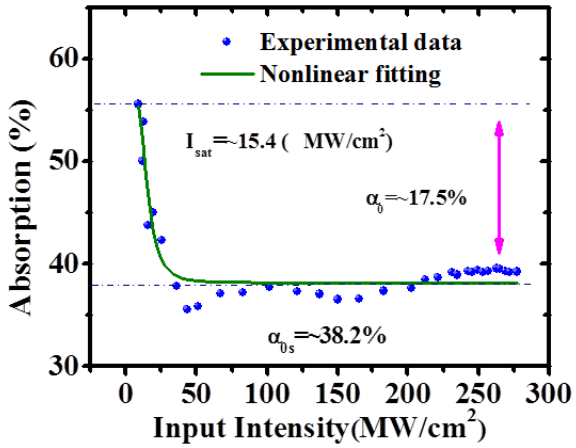

Figure 3. Measured nonlinear absorbance of the TI-PCF SA device.

The laser source used was homebuilt mode-locked oscillator with 5 MHz repetition rate and 150 ps pulse duration, which operating at ~1064 nm. The date obtained from the experiment was then fitted according to

$$\alpha(I) = \alpha_0 \left(1 + \frac{I}{I_{\text{sat}}}\right)^{-1} + \alpha_{ns} \quad (1)$$

where I was the input laser intensity, I_{sat} was the saturable intensity, $\alpha(I)$ was the intensity-dependent absorption coefficient, and α_0 and α_{ns} were the modulation depth and the non-saturable loss, respectively. The results gave a saturable intensity of ~15.4 MW/cm^2, a modulation depth of ~17.5%, and a non-saturable loss of ~38.2%. The saturable intensity of the TI-PCF SA was comparative with

53 MW/cm^2 of TI: Bi_2Se_3 deposited onto fiber end facet [24] and 12 MW/cm^2 of TI: Bi_2Se_3 embedded into PVA film [30]. On the other hand, the modulation depth of the TI-PCF SA would be high enough for stable femtosecond pulse mode-locking, considering that another TI SA with 1.7% modulation depth has demonstrated the HML according to a recent report by Z. Luo *et al.* [27].

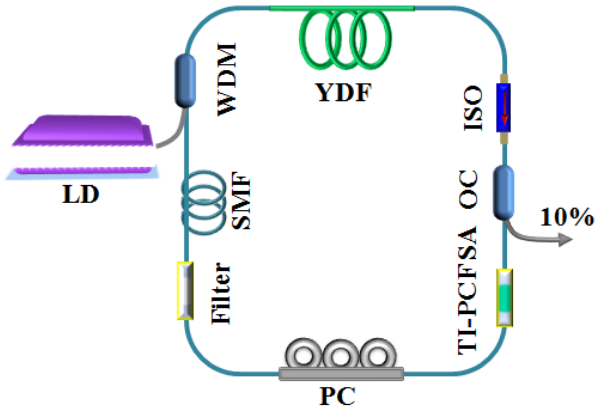

Figure 4. Schematic diagram of the fiber ring laser.

Our fiber laser was schematically shown in Figure 4. The laser was pumped by a 976 nm pump laser through a wavelength division multiplexer (WDM), and the output of the laser was coupled through a 10% fiber optical coupler (OC). A segment of ~3.4 m YDF with absorption of 250 dB/m@975 nm was used as the gain medium. A polarization independent isolator (ISO) was used to ensure the unidirectional operation of the ring laser cavity, and a three-spool polarization controller (PC) was employed to adjust the cavity birefringence. A bandwidth filter with a central wavelength of 1064 nm and 3 dB bandwidth of ~5 nm was inserted into the cavity. A total length of ~180 m HI-1060 Flex single mode fiber (SMF) was also incorporated to the cavity. The total cavity length was ~185 m. The monitoring of the output temporal pulse trains and optical spectrum were performed using a 20-GHz mixed signal oscilloscope (Tektronix MSO72004C) with a 45-GHz photo-detector (Newport 1014) and an optical spectrum analyzer (OSA, AQ6370B) with a minimum resolution of 0.02 nm, respectively. The pump power and output power were monitored by a photodiode power meter (COHERENT). In addition, the radio frequency (RF) spectrum of the fundamental mode-locking was measured by a Mixed Domain Oscilloscope (Tektronix MDO4034B-3).

3. Experimental Results and Discussion

3.1. Fundamental Mode-Locking

Continuous wave operation occurred at a pump power of ~76 mW. The stable operation in fundamental mode locking was observed up to the ~112 mW of pump power after careful adjustment of the PC, as shown in Figure 5a. The pulse train had a fundamental cavity frequency ~1.11 MHz, which was determined by the ~185 m cavity length. As depicted in the inset of Figure 5a, the full width at half maximum (FWHM) of the single pulse was ~2.33 ns. Figure 5b showed the typical spectrum of mode-locked pulses, it was centered at ~1062.27 nm with a 3 dB bandwidth of ~0.80 nm. In addition, the typical characteristics of steep spectral edges indicated that the mode-locked pulses

have been shaped to dissipative solitons, which are found exclusively in all normal-dispersion lasers, such as ytterbium-doped all-fiber laser [55]. The corresponding RF spectrum of the laser was shown Figure 5c, and it was clearly shown that the repetition rate of the pulse train was ~1.11 MHz. The electrical signal-to-noise ratio (SNR) was ~61 dB measured with 20 kHz resolution bandwidth (RBW). It was introduced more additional linear dispersion and nonlinearity into the all-normal-dispersion cavity due to the extra fiber of ~185 m, which required for the extreme pulse broadening [56,57]. Thus, it was reasonable that the single pulse here was larger than 2 ns.

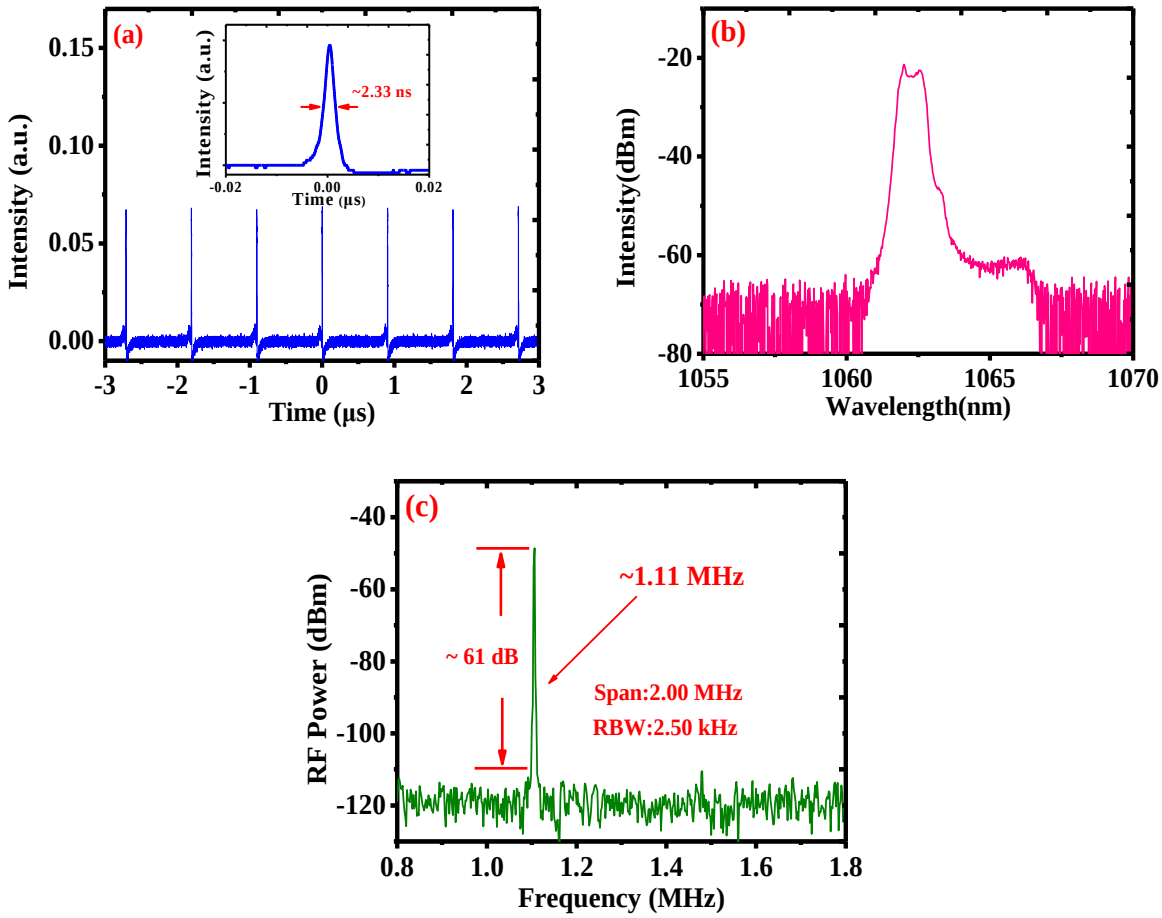

Figure 5. (**a**) Fundamental mode-locking pulse train. Inset: single pulse width. (**b**) Corresponding spectrum. (**c**) Fundamental frequency signal.

3.2. Harmonic Mode-Locking

For a passively harmonic mode-locked laser, splitting of pulses usually occurred before the attainment of nearly equal-spaced and self-organized pulse train. By increasing the pump power and adjusting the orientation of PC carefully, splitting of pulse occurred owing to the cavity pulse peak clamping effect. This process was similar to the soliton operation state in the fiber lasers with net negative cavity group-velocity dispersion [58]. The multiple pulses then rearranged themselves automatically, and all pulses were equally spaced in the cavity. Firstly, 2nd-order HML was observed at the pump power of ~127 mW by changing the PC, as shown in Figure 6a. The corresponding RF spectrum was measured, which was given in Figure 6e. It could be seen that the SNR of 2nd order

HML was ~ 45 dB, and its repetition rate was ~2.21 MHz (RBW was 2.50 kHz). The harmonic number could also be enlarged only by increasing the pump power slightly in our experiment, the pulse trains of the 3rd (Figure 6b), 4th (Figure 6c) and 5th (Figure 6d) order HML could be obtained under the pump powers of ~131 mW, ~140 mW, ~149 mW, respectively. In addition, the corresponding RF spectra of the 3rd (the repetition rate of ~3.32 MHz), 4th (the repetition rate of ~4.42 MHz) and 5th (the repetition rate of ~5.53 MHz) order HML were given in Figure 6f–h with the corresponding SNRs of ~ 43 dB, ~ 42 dB and ~ 42 dB, respectively. Finally, an inverse progress was explored. When the pump power was decreased to ~137 mW, the 4th order HML appeared again, then the 3th and 2nd order HML appeared in turn under a little below the previous pump powers due to the hysteresis phenomena of HML [59]. Similar to the previous work [60], the multi-wavelength mode-locked pulses were also observed in the experiment.

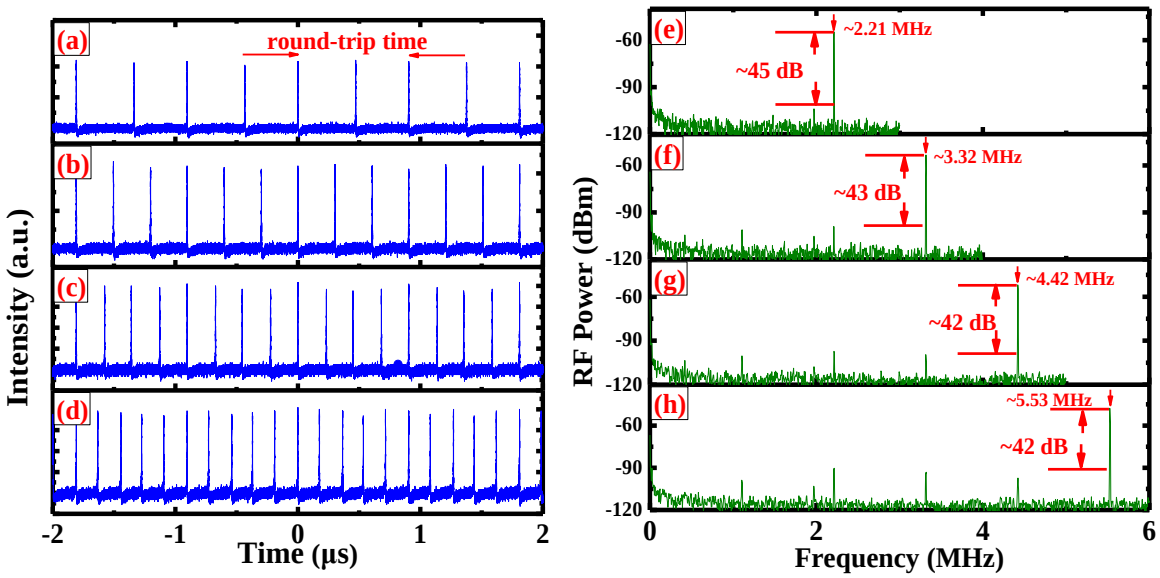

Figure 6. Pulse trains for (**a**) 2nd HML, (**b**) 3rd HML, (**c**) 4th HML and (**d**) 5th HML as well as the corresponding RF-spectra for (**e**) 2nd HML, (**f**) 3rd HML, (**g**) 4th HML and (**h**) 5th HML, respectively.

Further increasing the pump power to ~324 mW, a noticeable transition from a bunched state of pulses to high-order HML could be repeatedly achieved by tuning the orientation of PC, as illustrated in Figure 7a–e. It was clearly shown that the bunch of pulses expanded gradually and occupied the whole cavity regularly, leading to the formation of a high-order HML state eventually (shown in Figure 7e. The Figure 7f indicated that the FWHM of a single pulse in HML was ~575.80 ps. Figure 7g showed the typical output optical spectra of initial state (corresponding to the oscilloscope trace of Figure 7a and final state (corresponding to the oscilloscope trace of Figure 7e. The HML had a central wavelength of 1065.4 nm and a 3-dB spectral bandwidth of 1.51 nm. The corresponding RF spectrum was also measured, as shown in Figure 7h. The SNR of the high-order HML was ~ 38 dB, and the final repetition rate was ~28.73 MHz, corresponding to the 26th harmonic. Here we use photonic crystal fiber filled with TI:Bi_2Te_3 nanosheets solution as saturable absorber to achieve harmonic mode-locking. Another way [61] like single-wall carbon nanotube (SWCNT)-doped

polyvinyl alcohol (PVA)-based as saturable absorber through using either all-physical-contact (PC) or all-angled-physical-contact (APC) connectors can also be used.

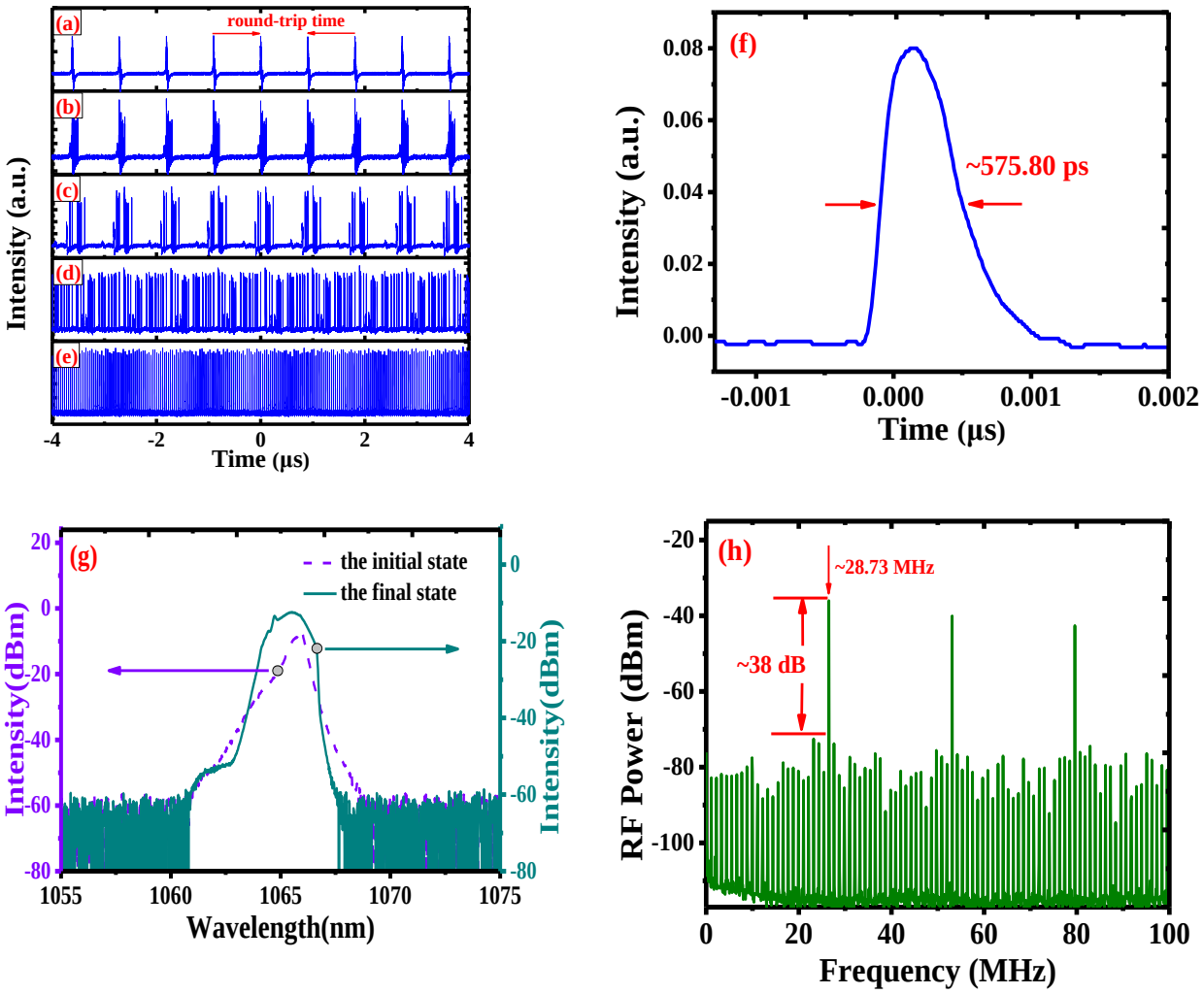

Figure 7. (**a**–**e**) the transition from a bunched state to the 26th-order HML. (**f**) the single pulse of 26th-order HML. (**g**) Optical spectra of initial and final state. (**h**) The corresponding RF spectrum of 26th-order HML.

4. Conclusions

As a summary, a TI-PCF SA device was firstly demonstrated, which possessed some unique advantages, such as single mode operation, nonlinearity enhancement, low insertion loss, all-fiber configuration, longer action length. Employing this SA device, an ytterbium-doped all-fiber laser was constructed and the evanescent wave mode-locking operation was achieved. Not only stable fundamental mode-locking and low order HML, but also the transition dynamics from a bunched state of pulses to high order HML were demonstrated. Our experimental results demonstrate a new scheme for ultra-fast laser mode-locking application.

Acknowledgments

This research was Supported by the NSFC (61275144), Natural science fund of Guangdong province (S2013010012235), the foundation for scientific and technical innovation in Higher Education of Guangdong (2013KJCX0161), the Improvement and Development Project of Shenzhen Key Lab (ZDSY20120612094924467), the Science and technology project of Shenzhen City (JCYJ20120613172042264, JCYJ20130329142040731), Natural Science Foundation of SZU (No.201221).

Author Contributions

Writing of paper: Yu-Shan Chen. Comments and feedback: Yu-Shan Chen. Experimental investigations: Pei-Guang Yan, Yu-Shan Chen, Hao Chen, Ai-Jiang Liu and Shuang-Chen Ruan. Schemes and design of investigations: Pei-Guang Yan.

Conflict of Interest

The authors declare no conflict of interest.

References

1. Zhang, H.; Tang, D.; Knize, R.J.; Zhao, L.; Bao, Q.; Loh, K.P. Graphene mode locked, wavelength-tunable, dissipative soliton fiber laser. *Appl. Phys. Lett*. **2010**, *96*, 111–112.
2. Wise, F.W.; Chong, A.; Renninger, W.H. High-energy femtosecond fiber lasers based on pulse propagation at normal dispersion. *Laser Photon. Rev.* **2008**, *2*, 58–73.
3. Kobtsev, S.; Kukarin, S.; Fedotov, Y. Ultra-low repetition rate mode-locked fiber laser with high-energy pulses. *Opt. Express* **2008**, *16*, 21936–21941.
4. McFerran, J.J. Echelle spectrograph calibration with a frequency comb based on a harmonically mode-locked fiber laser: A proposal. *Appl. Opt*. **2009**, *48*, 2752–2759.
5. Mikulla, B.; Leng, L.; Sears, S.; Collings, B.C.; Arend, M.; Bergman, K. Broad-Band High-Repetition-Rate Source for Spectrally Sliced WDM. *IEEE Photon. Technol. Lett*. **1999**, *11*, 418–420.
6. Zhang, Z.X.; Zhan, L.; Yang, X.X.; Luo, S.Y.; Xia, Y.X. Passive harmonically mode-locked erbium-doped fiber laser with scalable repetition rate up to 1.2 GHz. *Laser Phys. Lett*. **2007**, *4*, 592.
7. Amrani, F.; Haboucha, A.; Salhi, M.; Leblond, H.; Komarov, A.; Grelu, Ph.; Sanchez, F. Passively mode-locked erbium-doped double-clad fiber laser operating at the 322nd harmonic. *Opt. Lett*. **2009**, *34*, 2120–2122.
8. Zhu, X.J.; Wang, C.H.; Liu, S.X.; Zhang, G.J. Tunable High-Order Harmonic Mode-Locking in Yb-Doped Fiber Laser With All-Normal Dispersion. *Photon. Technol. Lett*. **2012**, *24*, 754–756.
9. Peng, J.; Zhan, L.; Luo, S.; Shen, Q. Passive Harmonic Mode-Locking of Dissipative Solitons in a Normal-Dispersion Er-Doped Fiber Laser. *J. Lightw. Technol*. **2013**, *31*, 3009–3014.
10. Chen, H.R.; Lin, K.H.; Tsai, C.Y.; Wu, H.H.; Wu, C.H.; Chen, C.H.; Chi, Y.C.; Lin, G.R.; Hsieh, W.F. 12 GHz passive harmonic mode-locking in a 1.06 μm semiconductor optical amplifier-based fiber laser with figure-eight cavity configuration. *Opt. Lett*. **2013**, *38*, 845–847.

11. Jun, C.S.; Choi, S.Y.; Rotermund, F.; Kim, B.Y.; Yeom, D. Toward higher-order passive harmonic mode-locking of a soliton fiber laser. *Opt. Lett*. **2012**, *37*, 1862–1864.
12. Jun, C.S.; Im, J.H.; Yoo, S.H.; Choi, S.Y.; Rotermund, F.; Yeom, D.; Kim, B.Y. Low noise GHz passive harmonic mode-locking of soliton fiber laser using evanescent wave interaction with carbon nanotubes. *Opt. Express* **2011**, *19*, 19775–19780.
13. Mou, C.B.; Arif, R.; Rozhin, A.; Turitsyn, S. Passively harmonic mode locked erbium doped fiber soliton laser with carbon nanotubes based saturable absorber. *Opt. Mater. Express* **2012**, *2*, 884–890.
14. Sotor, J.; Sobon, G.; Macherzynski, W.; Abramski, K.M. Harmonically mode-locked Er-doped fiber laser based on a Sb_2Te_3 topological insulator saturable absorber. *Laser Phys. Lett*. **2014**, *11*, 055102.
15. Sobon, G.; Sotor, J.; Abramski, K.M. Passive harmonic mode-locking in Er-doped fiber laser based on graphene saturable absorber with repetition rates scalable to 2.22 GHz. *Appl. Phys. Lett*. **2012** ,*100*, 161109.
16. Huang, S.S.; Wang, Y.G.; Yan, P.G.; Zhang, G.L.; Zhao, J.Q.; Li, H.Q.; Lin, R.Y. High order harmonic modelocking in an allnormaldispersion Ybdoped fiber laser with a graphene oxide saturable absorber. *Laser Phys*. **2014**, *24*, 015001.
17. Martinez, A.; Sun, Z. Nanotube and graphene saturable absorbers for fibre lasers. *Nat. Photon.* **2013**, *7*, 842–845.
18. Lin, G.; Lin, Y. Directly exfoliated and imprinted graphite nano-particle saturable absorber for passive mode-locking erbium-doped fiber laser. *Laser Phys. Lett.* **2011**, *8*, 880.
19. Lin, Y.H.; Chi, Y.C.; Lin, G.R. Nanoscale charcoal powder induced saturable absorption and mode-locking of a low-gain erbium-doped fiber-ring laser. *Laser Phys. Lett.* **2013**, *10*, 055105.
20. Qi, X.L.; Zhang, S.C. Topological insulators and superconductors. *Rev. Mod. Phys.* **2011**, *83*, 1057.
21. Hasan, M.Z.; Kane, C.L. Colloquium: Topological insulators. *Rev. Mod. Phys.* **2010**, *82*, 3045.
22. Sotor, J.; Sobon, G.; Abramski, K.M. Sub-130 fs mode-locked er-doped fiber laser based on topological insulator. *Opt. Express* **2014**, *22*, 13244–13249.
23. Zhao, C.; Zhang, H.; Qi, X.; Chen, Y.; Wang, Z.; Wen, S.; Tang, D. Ultra-short pulse generation by a topological insulator based saturable absorber. *Appl. Phys. Lett.* **2012**, *101*, 211106.
24. Luo, Z.; Huang, Y.; Weng, J.; Cheng, H.; Lin, Z.; Xu, B.; Cai, Z.; Xu, H. 1.06 μm q-switched ytterbium-doped fiber laser using few-layer topological insulator Bi_2Se_3 as a saturable absorber. *Opt. Express* **2013**, *21*, 29516–29522.
25. Yu, Z.; Song, Y.; Tian, J.; Dou, Z.; Guoyu, H.; Li, K.; Li, H.; Zhang, X. High-repetition-rate q-switched fiber laser with high quality topological insulator Bi_2Se_3 film. *Opt. Express* **2014**, *22*, 11508–11515.
26. Chen, Y.; Zhao, C.; Huang, H.; Chen, S.; Tang, P.; Wang, Z.; Lu, S.; Zhang, H.; Wen, S.; Tang, D. Self-Assembled Topological Insulator: Bi_2Se_3 Membrane as a Passive Q-Switcher in an Erbium-Doped Fiber Laser. *J. Lightw. Technol*. **2013**, *31*, 2857–2863.
27. Luo, Z.C.; Liu, M.; Liu, H.; Zheng, X.W.; Luo, A.P.; Zhao, C.J.; Zhang, H.; Wen, S.C.; Xu, W.C. 2 GHZ passively harmonic mode-locked fiber laser by a microfiber-based topological insulator saturable absorber. *Opt. Lett.* **2013**, *38*, 5212–5215.

28. Zhao, C.; Zou, Y.; Chen, Y.; Wang, Z.; Lu, S.; Zhang, H.; Wen, S.; Tang, D. Wavelength-tunable picosecond soliton fiber laser with topological insulator: Bi_2Se_3 as a mode locker. *Opt. Express* **2012**, *20*, 27888–27895.
29. Luo, Z.; Liu, C.; Huang, Y.; Wu, D.; Wu, J.; Xu, H.; Cai, Z.; Lin, Z.; Sun, L.; Weng, J. Topological-insulator passively q-switched double-clad fiber laser at 2 μm wavelength. *IEEE J. Sel. Top. Quant. Electron.* **2014**, *20*, 0902708.
30. Liu, H.; Zheng, X.W.; Liu, M.; Zhao, N.; Luo, A.P.; Luo, Z.C.; Xu, W.C.; Zhang, H.; Zhao, C.J.; Wen, S.C. Femtosecond pulse generation from a topological insulator mode-locked fiber laser. *Opt. Express* **2014**, *22*, 6868–6873.
31. Chen, Y.; Zhao, C.; Chen, S.; Du, J.; Tang, P.; Jiang, G.; Zhang, H.; Wen, S.; Tang, D. Large energy, wavelength widely tunable, topological insulator q-switched erbium-doped fiber laser. *IEEE J. Sel. Top. Quant. Electron.* **2014**, *20*, 315–322.
32. Lee, J.; Koo, J.; Jhon, Y.-M.; Lee, J.H. A femtosecond pulse erbium fiber laser incorporating a saturable absorber based on bulk-structured Bi_2Se_3 topological insulator. *Opt. Express* **2014**, *22*, 6165–6173.
33. Lin, Y.H.; Yang, C.Y.; Lin, S.F.; Tseng, W.H.; Bao, Q.; Wu, C.-I.; Lin, G.-R. Soliton compression of the erbium-doped fiber laser weakly started mode-locking by nanoscale p-type Bi_2Te_3 topological insulator particles. *Laser Phys. Lett.* **2014**, *11*, 055107.
34. Yan, P.; Lin, R.; Ruan, S.; Liu, A.; Chen, H.; Zheng, Y.; Chen, S.; Guo, C.; Hu, J. A practical topological insulator saturable absorber for mode-locked fiber laser. *Sci. Rep.***2015**, *5*, 8690.
35. Yan, P.; Lin, R.; Ruan, S.; Liu, A.; Chen, H. A 2.95 GHz, femtosecond passive harmonic mode-locked fiber laser based on evanescent field interaction with topological insulator film. *Opt. Express* **2015**, *23*, 154–164.
36. Yan, P.; Lin, R.; Chen, H.; Zhang, H.; Liu, A.; Yang, H.; Ruan, S. Topological insulator solution filled in photonic crystal fiber for passive mode-locked fiber laser. *IEEE Photon. Tech. Lett.* **2015**, *27*, 264–267.
37. Huang, S.; Wang, Y.; Yan, P.; Zhao, J.; Li, H.; Lin, R. Tunable and switchable multi-wavelength dissipative soliton generation in a graphene oxide mode-locked Yb-doped fiber laser. *Opt. Express* **2014**, *22*, 11417–11426.
38. Lin, R.Y.; Wang, Y.G.; Yan, P.G.; Zhang, G.-L.; Zhao, J.-Q.; Li, H.Q.; Huang, S.S.; Cao, G.Z.; Duan, J.-A. Bright and dark square pulses generated from a graphene-oxide mode-locked ytterbium-doped fiber laser. *Photon. J. IEEE.* **2014**, *6*, 1–8.
39. Huang, S.; Wang, Y.; Yan, P.; Zhao, J.; Li, H.; Lin, R. Tunable and switchable multi-wavelength dissipative soliton generation in a graphene oxide mode-locked Yb-doped fiber laser. *Optics express* **2014**, *22*, 11417–11426.
40. Yan, P.; Liu, A.; Chen, Y.; Chen, H.; Ruan, S.; Guo, C.; Chen, S.; Li, I; Yang, H.; Hu, J.; Cao, G. Microfiber-based WS_2-film saturable absorber for ultra-fast photonics. *Opt. Mater. Express* **2015**, *5*, 479–489.
41. Boguslawski, J.; Sotor, J.; Sobon, G.; Tarka, J.; Jagiello, J.; Macherzynski, W.; Lipinska, L.; Abramski, K.M. Mode-locked er-doped fiber laser based on liquid phase exfoliated Sb_2Te_3 topological insulator. *Laser Phys.* **2014**, *24*, 105111.

42. Bernard, F.; Zhang, H.; Gorza, S.P.; Emplit, P. Towards mode-locked fiber laser using topological insulators. In Proceedings of the Nonlinear Photonics, Colorado Springs, CO, USA, 17–21 June 2012.
43. Bansal, N.; Kim, Y.S.; Edrey, E.; Brahlek, M.; Horibe, Y.; Iida, K.; Tanimura, M.; Li, G.-H.; Feng, T.; Lee, H.-D. Epitaxial growth of topological insulator Bi_2Se_3 film on Si (111) with atomically sharp interface. *Thin Solid Film.* **2011**, *520*, 224–229.
44. Jung, M.; Lee, J.; Koo, J.; Park, J.; Song, Y.-W.; Lee, K.; Lee, S.; Lee, J.H. A femtosecond pulse fiber laser at 1935 nm using a bulk-structured Bi_2Se_3 topological insulator. *Opt. Express* **2014**, *22*, 7865–7874.
45. Chen, Y.; Wu, M.; Tang, P.; Chen, S.; Du, J.; Jiang, G.; Li, Y.; Zhao, C.; Zhang, H.; Wen, S. The formation of various multi-soliton patterns and noise-like pulse in a fiber laser passively mode-locked by a topological insulator based saturable absorber. *Laser Phys. Lett.* **2014**, *11*, 055101.
46. Zhao, N.; Liu, M.; Liu, H.; Zheng, X.-W.; Ning, Q.-Y.; Luo, A.-P.; Luo, Z.-C.; Xu, W.-C. Dual-wavelength rectangular pulse Yb-doped fiber laser using a microfiber-based graphene saturable absorber. *Opt. Express* **2014**, *22*, 10906–10913.
47. Luo, Z.; Zhou, M.; Wu, D.; Ye, C.; Weng, J.; Dong, J.; Xu, H.; Cai, Z.; Chen, L. Graphene-induced nonlinear four-wave-mixing and its application to multiwavelength q-switched rare-earth-doped fiber lasers. *J. Lightw. Technol.* **2011**, *29*, 2732–2739.
48. Choi, S.Y.; Cho, D.K.; Song, Y.-W.; Oh, K.; Kim, K.; Rotermund, F.; Yeom, D.-I. Graphene-filled hollow optical fiber saturable absorber for efficient soliton fiber laser mode-locking. *Opt. Express* **2012**, *20*, 5652–5657.
49. Knight, J.C.; Broeng, J.; Birks, T.A.; Russell, P.S.J. Photonic band gap guidance in optical fibers. *Science* **1998**, *282*, 1476–1478.
50. Liu, Z.B.; He, X.; Wang, D. Passively mode-locked fiber laser based on a hollow-core photonic crystal fiber filled with few-layered graphene oxide solution. *Opt. Lett.* **2011**, *36*, 3024–3026.
51. Lin, Y.H.; Yang, C.Y.; Liou, J.H.; Yu, C.P.; Lin, G.R. Using graphene nano-particle embedded in photonic crystal fiber for evanescent wave mode-locking of fiber laser. *Opt. Express* **2013**, *21*, 16763–16776.
52. Zhao, J.; Ruan, S.; Yan, P.; Zhang, H.; Yu, Y.; Wei, H.; Luo, J. Cladding-filled graphene in a photonic crystal fiber as a saturable absorber and its first application for ultrafast all-fiber laser. *Opt. Eng.* **2013**, *52*, 106105–106105.
53. Liu, M.; Zhao, N.; Liu, H.; Zheng, X.-W.; Luo, A.-P.; Luo, Z.-C.; Xu, W.-C.; Zhao, C.-J.; Zhang, H.; Wen, S.-C. Dual-wavelength harmonically mode-locked fiber laser with topological insulator saturable absorber. *IEEE Photon. Technol. Lett.* **2014**, *26*, 983–986.
54. Lu, S.B.; Zhao, C.J.; Zou, Y.H.; Chen, S.Q.; Chen, Y.; Li, Y.; Zhang, H.; Wen, S.C.; Tang, D.Y. Third order nonlinear optical property of Bi_2Se_3. *Opt. Express* **2013**, *21*, 2072–2082.
55. Grelu, P.; Akhmediev, N. Dissipative solitons for mode-locked lasers. *Nat. Photon.* **2012**, *6*, 84–92.
56. Kelleher, E.J.R.; Travers, J.C.; Ippen, E.P.; Sun, Z.; Ferrari, A.C.; Popov, S.V.; Taylor, J.R. Generation and direct measurement of giant chirp in a passively mode-locked laser. *Opt. Lett.* **2009**, *34*, 3526–3528.

57. Kelleher1, E.J.R.; Travers, J.C.; Sun, Z.; Rozhin, A.G.; Ferrari, A.C.; Popov, S.V.; Taylor, J.R. Nanosecond-pulse fiber lasers mode-locked with nanotubes. *Appl. Phys. Lett.* **2009**, *95*, 111108.
58. Tang, D.Y.; Zhao, L.M.; Zhao, B.; Liu, A.Q. Mechanism of multisoliton formation and soliton energy quantization in passively mode-locked fiber lasers. *Phys. Rev. A.* **2005**, *72*, 43816.
59. Liu, X. Hysteresis phenomena and multipulse formation of a dissipative system in a passively mode-locked fiber laser. *Phys. Rev. A.* **2010**, *81*, 23811.
60. Guo, B.; Yao, Y.; Tian, J.; Zhao, Y.; Liu, S.; Li, M.; Quan, M. Observation of bright-dark soliton pair in a mode-locked fiber laser with topological insulator. *IEEE Photon. Technol. Lett*. **2015**, *27*, 701–704.
61. Cheng, K.N.; Lin, Y.H.; Yamashita, S.; Lin, G.R. Harmonic order-dependent pulsewidth shortening of a passively mode-locked fiber laser with a carbon nanotube saturable absorber. *Photonics Journal, IEEE.* **2012**, *4*, 1542–1552.

© 2015 by the authors; licensee MDPI, Basel, Switzerland. This article is an open access article distributed under the terms and conditions of the Creative Commons Attribution license (http://creativecommons.org/licenses/by/4.0/).